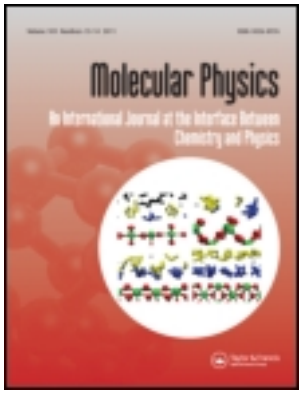

Molecular Physics
Publication details, including instructions for authors and subscription information:
http://www.tandfonline.com/loi/tmph20

Excess entropy of water in a supercooled solution of salt

P. Gallo [a] , D. Corradini [b] & M. Rovere [a]

[a] Dipartimento di Fisica, Università Roma Tre, Via della Vasca Navale 84, Roma, Italy

[b] Center for Polymer Studies and Department of Physics, Boston University, Boston, MA 02215, USA

Available online: 18 Nov 2011

To cite this article: P. Gallo, D. Corradini & M. Rovere (2011): Excess entropy of water in a supercooled solution of salt, Molecular Physics, 109:23-24, 2969-2979

To link to this article: http://dx.doi.org/10.1080/00268976.2011.635605

Molecular Physics
Vol. 109, Nos. 23–24, 10 December–20 December 2011, 2969–2979

INVITED ARTICLE

Excess entropy of water in a supercooled solution of salt

P. Gallo[a], D. Corradini[b] and M. Rovere[a]*

[a]*Dipartimento di Fisica, Università Roma Tre, Via della Vasca Navale 84, Roma, Italy;*
[b]*Center for Polymer Studies and Department of Physics, Boston University, Boston MA 02215, USA*

(*Received 1 August 2011; final version received 21 October 2011*)

We consider the relationship between the excess entropy and anomalies of water. We investigate by molecular dynamics simulations the thermodynamic region of supercooled water and a supercooled aqueous solution with NaCl at a salt concentration of 0.67 mol kg^{-1}. The TIP4P potential model displays, as already established, in pure water and in solution a phase diagram with a liquid–liquid critical point. We explore how the two-body excess entropy calculated from the radial distribution functions is an indicator of density and structural anomalies of supercooled liquid water, both in the pure system and in the NaCl(aq). The two-body excess entropy shows a peculiar behaviour associated with the density anomaly and structural changes in water as revealed by the radial distribution functions. The signature of a change in the structural relaxation of water from fragile to strong is also found by examining the behaviour of the excess entropy at decreasing temperature.

Keywords: ionic aqueous solutions; excess entropy; supercooled water; anomalies of water; structure of supercooled water

1. Introduction

Water shows a number of unusual properties which have stimulated for a long time a huge amount of experimental, computational and theoretical work, owing to the relevance of water in phenomena taking place in physics, chemistry, and biology. The most well-known thermodynamic anomaly of liquid water is the behaviour of its density. At fixed pressure the volume decreases with decreasing temperature, as usual for liquids, but below a temperature of maximum density (TMD) water expands upon cooling, the TMD at ambient pressure having the value of 4°C.

The anomalies of liquid water become more pronounced upon supercooling. Thermodynamic functions of water, like isothermal compressibility and specific heat, show a strong increase upon supercooling [1–9]. Extrapolation obtained by power law fits indicates an apparent divergence at a temperature of −45°C, just below the temperature of homogeneous nucleation [3].

Based on computer simulation results obtained with the ST2 water model [10,11] the divergence of these thermodynamic quantities was attributed to the possibility that water upon supercooling shows a liquid–liquid coexistence terminating in a liquid–liquid critical point (LLCP). This interpretation is an alternative to other hypotheses, such as the singularity free scenario [12] and the more recent interpretation based on a disorder to order transition [13].

Liquid–liquid equilibrium is a typical phenomenon of fluid mixtures but in recent years, in pure substances a coexistence has been found between two liquid phases, see for instance the discussion in [14]. Computer simulations show evidence for a liquid–liquid transition in systems such as silicon [15–18] and silica [19–22]. In these cases, as in water, the phenomenon would take place in the metastable phase of the supercooled liquid, if the formation of the stable crystalline phase can be avoided.

The hypothesis of a metastable LLCP in water is supported by the experimental determination of different coexisting phases of glassy water, the so-called polyamorphism of water. The high density amorphous (HDA) and low density amorphous (LDA) phases would transform at increasing temperature in the corresponding high density liquid (HDL) and low density liquid (LDL) phases [1,2]. In the metastable liquid the coexistence curve would terminate at a critical point. A first-order phase transition among HDA and LDA has been determined by experiments [23–26], instead LDL and HDL are in the region of temperature and pressure hampered by crystallization

*Corresponding author. Email: rovere@fis.uniroma3.it

ISSN 0026–8976 print/ISSN 1362–3028 online

http://dx.doi.org/10.1080/00268976.2011.635605
http://www.tandfonline.com

in real water. From available measurements on supercooled water [27,28] the LLCP was proposed to be located at around $T = 220\,\mathrm{K}$ and $P = 100\,\mathrm{MPa}$.

After the first computation with the ST2 model a number of computer simulations performed with different potentials for water found the existence of the LDL–HDL coexistence and estimated the position of the LLCP, see for example [1,2,29–36].

Due to the difficulties in performing experiments on supercooled pure water, in recent years computer and experiments have focused on different routes to observe the liquid–liquid coexistence. Water can be studied in confinement or in solutions to prevent crystallization.

In ionic aqueous solutions there is experimental evidence that anomalies of water are preserved [37,38] and polyamorphic phase transitions are measured [39,40]. This motivated our recent computer simulation studies on aqueous solutions of salts [34,41–43].

We performed a detailed analysis of the thermodynamic properties of aqueous solutions of NaCl at various salt concentrations upon supercooling. In particular for the concentration of $0.67\,\mathrm{mol\,kg^{-1}}$ it was estimated that the LLCP is located in a position where it could be reachable by experiments [34] since the phase diagram is shifted with respect to the bulk.

In this paper we focus on the $0.67\,\mathrm{mol\,kg^{-1}}$ NaCl(aq) and consider a further quantity whose behaviour can indicate the presence of anomalies in the liquid. This quantity is the excess entropy. As shown in the literature, the excess entropy under the assumption that pair forces are the most relevant can be obtained from the integration of the pair correlation functions [44]. We will calculate the excess entropy from the structure of the TIP4P water and the NaCl(aq) in the region of supercooling to explore how this quantity can be related to the anomalous behaviour of water and to determine the effect of the ions on it.

In Section 2 we will introduce the model for the liquid water and the liquid ionic solutions and the method adopted. In Section 3 we recall some of the thermodynamic results obtained on these systems to show the effect of the ions on the behaviour of water. In Section 4 we present the calculation of the excess entropy and we will discuss the results. Section 5 is devoted to conclusions.

2. Models and methods

The results that we will present have been obtained by Molecular Dynamics (MD) simulations of water and the NaCl(aq) solution at a concentration of $0.67\,\mathrm{mol\,kg^{-1}}$. We adopted for describing water the TIP4P site potential, where the molecule is considered rigid and composed of four sites [45]. Two sites represent hydrogens (H) and are positively charged. They are connected to a neutral oxygen (O) site, whose negative charge is shifted and attributed to the fourth site (X). The OH bond length is 0.9572 Å, the angle between the two bonds is $\theta = 104.5^\circ$. The X site lies in the molecular plane shifted by 0.15 Å from the oxygen, and the OX bond forms an angle $\theta/2$ with the OH bonds. Each H site has a charge of $0.52e$ and the X charge is $-1.04e$. The interactions between the sites of the water molecule, the ions and water sites with ions is described by combining coulombic and the Lennard-Jones (LJ) potentials

$$u_{\alpha\beta}(r) = \frac{q_\alpha q_\beta}{r_{\alpha\beta}} + 4\epsilon_{\alpha\beta}\left[\left(\frac{\sigma_{\alpha\beta}}{r_{\alpha\beta}}\right)^{12} - \left(\frac{\sigma_{\alpha\beta}}{r_{\alpha\beta}}\right)^{6}\right]. \qquad (1)$$

The LJ parameters for ions were optimized for use with TIP4P water by the Jensen and Jorgensen model [46]. They found that the parameters reproduce well the structural characteristics and free energies of hydration of the ions. The ion–ion and the ion–water LJ parameters were calculated by the use of the geometrical mixing rules $\epsilon_{\alpha\beta} = (\epsilon_{\alpha\alpha}\epsilon_{\beta\beta})^{1/2}$ and $\sigma_{\alpha\beta} = (\sigma_{\alpha\alpha}\sigma_{\beta\beta})^{1/2}$.

All the LJ parameters are reported in Table 1.

The simulations were performed for pure water, also called in the following bulk water, with $N_\mathrm{w} = 256$ molecules. The salt solution was simulated with $N_\mathrm{w} = 250$ water molecules, three Na^+; cations and three Cl^- anions.

Periodic boundary conditions were applied. The interaction potentials were truncated at $r_\mathrm{cut} = 9$ Å. The long-range electrostatic interactions were taken into account with the Ewald particle mesh method. The integration time step was fixed at 1 fs.

Table 1. Lennard-Jones parameters of the interactions between oxygen atoms in the TIP4P water molecule, between ions and between ions and oxygen. H and X sites of water interact only by Coulomb potential.

	ϵ (kJ mol^{-1})	σ (Å)
OO	0.649	3.154
NaNa	0.002	4.070
NaCl	0.079	4.045
ClCl	2.971	4.020
NaO	0.037	3.583
ClO	1.388	3.561

In order to study and compare the phase diagrams and structural properties of pure TIP4P water and the NaCl(aq), extensive sets of simulations were run for both systems [34,42]. The range of densities investigated spans from $\rho = 0.83\,\mathrm{g\,cm^{-3}}$ to $\rho = 1.10\,\mathrm{g\,cm^{-3}}$. The temperatures goes from $T = 350\,\mathrm{K}$ to $T = 190\,\mathrm{K}$. The Berendsen thermostat was used. Equilibration and production simulation times were progressively increased with decreasing temperature. The runs correspond to circa six years of single CPU time.

3. Thermodynamic results

As stated above in a recent simulation study [34] with extensive calculations we determined the phase diagrams of both the TIP4P water and the NaCl aqueous solution in the supercooled liquid region. In both systems the anomalous behaviour of water was evidenced in various thermodynamic properties. From the isotherms it was possible to determine the line of the mechanical stability (LMS) which is the locus of the points where the mechanical stability condition

$$\left(\frac{\partial V}{\partial P}\right)_T < 0 \tag{2}$$

is violated. The LMS represents the limiting value of the existence of the metastable liquid against the gas phase. In the case of pure water the LMS is the liquid spinodal line which emanates from the liquid–gas critical point. The TMD lines have been determined from the change of sign of the derivative $(\partial V/\partial T)_P$. From the analysis of the thermodynamic behaviour of the supercooled liquid the position of the LLCP was estimated. The Widom line, where the maxima of the response functions converge in approaching the LLCP from the single phase region [32,47], was also calculated. In Figure 1 the thermodynamic results, obtained in [34], are shown in the P–ρ plane. The changes determined by the ionic solute can be observed.

The LMS is slightly shifted to higher density, while at low densities the TMD line moves to lower temperature and avoids the LMS line as in pure water. We note a change in the TMD line of the solution, that it is shifted up in density. The shift is larger in the low density branch. The high density branch of the TMD solution crosses the corresponding branch of the bulk TMD line. This behaviour in the one phase region is reminiscent to that found in simulations of water confined in hydrophobic confinement [48–50].

The LLCP is shifted to lower density and higher temperatures in the solution. By matching the TMD line of bulk water obtained in simulation with the experimental branch measured, we have found that TIP4P water is able to reproduce fairly well the properties of real water with a rigid shift of the phase diagram of $+31\,\mathrm{K}$ in temperature and $-73\,\mathrm{MPa}$ in pressure.

Taking into account this shift and assuming that an analogous shift is present for the $0.67\,\mathrm{mol\,kg^{-1}}$ NaCl(aq), it was estimated that the LLCP of the real ionic solutions would be located at $T = 230\,\mathrm{K}$ and $P = -120\,\mathrm{MPa}$ [34]. These values are in a region that

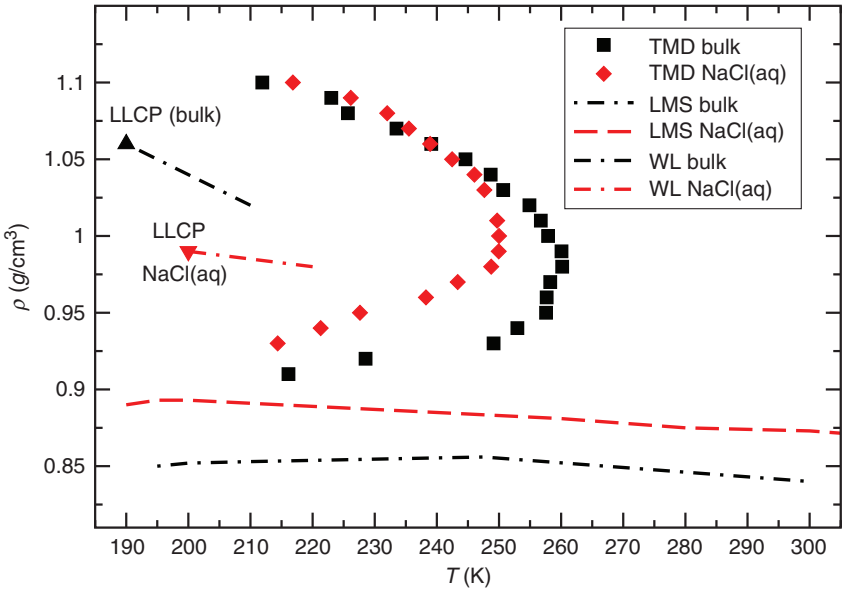

Figure 1. TMD lines, LMS lines, estimated positions of the LLCP in the (ρ, T) thermodynamic plane for bulk water and NaCl(aq). A portion of the Widom lines (WL) are also shown for both cases. Plotted in the ρ–T plane from data of [34].

appears possible to reach by experiments, in spite of the negative pressure, being slightly above the homogeneous nucleation [51,52].

4. Excess entropy from the structure

There have been numerous studies of the excess two-body entropy in liquids. Scaling relations between the excess entropy and transport properties were also investigated in different liquid systems with different model potentials [53–61]. In particular the behaviour of the excess entropy of water was found to be connected to the structural anomaly of the liquid [62,63] and to the liquid–liquid transition [64].

Excess entropy is defined as the difference between the entropy and the entropy of an ideal gas

$$S_{\mathrm{exc}} = S - S_{\mathrm{id}}. \tag{3}$$

For the excess entropy, an expansion in terms of n-body contributions represented by integrals on the n-particle distribution functions $g^n(r_1, \ldots, r_n)$ has been determined [44]. With the assumption that the main contribution to the particle interaction comes from the two-body terms, the excess entropy per particle $s_{\mathrm{exc}} = S_{\mathrm{exc}}/N$ can be calculated with the formula

$$s_{\mathrm{exc}} \approx s_2 = -2\pi\rho k_{\mathrm{B}} \int \{g(r)\ln[g(r)] - [g(r) - 1]\} r^2 \, \mathrm{d}r, \tag{4}$$

where $g(r)$ is the radial distribution function (RDF).

In the case of pure water the entropy is calculated for the centre of mass of the molecules which approximately coincides with the oxygen, so in Equation (4) the $g(r)$ is the oxygen–oxygen RDF.

For the salt solution Equation (4) must be modified to the more general formula

$$s_2 = -2\pi\rho k_{\mathrm{B}} \sum_{\alpha\beta} x_\alpha x_\beta \times \int \{g_{\alpha\beta}(r)\ln[g_{\alpha\beta}(r)] - [g_{\alpha\beta}(r) - 1]\} r^2 \mathrm{d}r, \tag{5}$$

where x_α is the concentration of the α component.

We calculated the two-body entropy with the RDF obtained in [42] for bulk water and the solution. We note that the TIP4P RDF compares well with experiments [65], as discussed for instance in [66].

In our case due to the low ion concentration the main contribution to s_2 in Equation (5) comes from the water structure. In Figure 2 we show the oxygen–oxygen RDF of the bulk water for $T = 190\,\mathrm{K}$ over a range of densities which starts from $\rho = 0.86\,\mathrm{g\,cm^{-3}}$ up to $\rho = 1.09\,\mathrm{g\,cm^{-3}}$. From Figure 1 it is evident that at increasing density the liquid moves from the low density to the high density region of the supercooled liquid. The main changes in the $g_{\mathrm{OO}}(r)$ take place in the region of the second peak. In HDL the second peak shifts to lower distances while its height decreases, and its shape broadens. As already discussed in [42] the differences between the LDL and HDL structure

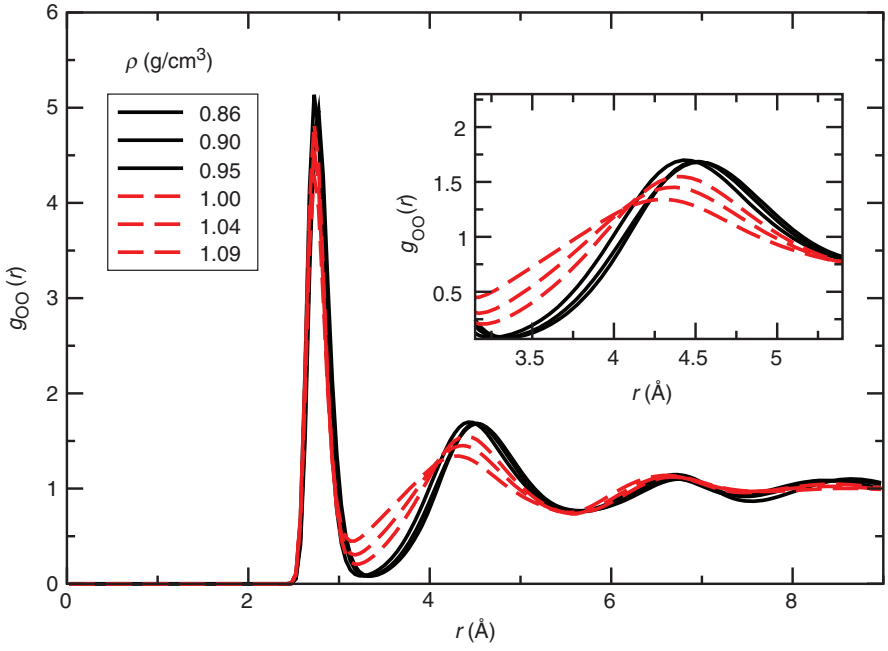

Figure 2. Oxygen–oxygen RDF of TI4P bulk water at $T = 190\,\mathrm{K}$ for various densities as indicated. The black bold curves indicate the LDL regime, while the red broken curves indicate the HDL regime. In the inset the same functions are reported on an enlarged scale in the region of the second shell. (Data from [42].)

found here are consistent with the experimental results reported in [65,67], where the transformation between the two forms of water were extensively analysed.

In our computer simulation at finite size we do not expect to observe a sharp transition between the two phases, but as seen in Figure 2 we can identify two regimes for the region between the first minimum and the second shell with a change between a LDL-like to a HDL-like structure between $\rho = 0.95\,\mathrm{g\,cm^{-3}}$ and $\rho = 1.00\,\mathrm{g\,cm^{-3}}$. In this range of density the system crosses the liquid–liquid spinodals.

In Figure 3 we show the oxygen–oxygen RDF of the NaCl(aq) for $T = 200\,\mathrm{K}$ over a range of densities which starts from $\rho = 0.90\,\mathrm{g\,cm^{-3}}$ up to $\rho = 1.09\,\mathrm{g\,cm^{-3}}$. Considering the location of the LLCP in the salt solution shown Figure 1, as before the RDF evolves from the LDL toward the HDL region with a change between the two regimes taking place between $\rho = 0.94\,\mathrm{g\,cm^{-3}}$ and $\rho = 0.98\,\mathrm{g\,cm^{-3}}$.

As shown in previous work [42,68] the presence of ions at the concentration considered here does not induce much change in the structure of water apart from the differences due to the shift in the phase diagram with a consequent different position of the LLCP.

We note, as a technical point, that from Figures 2–3 the accuracy of our RDF calculations is apparent, owing to the long runs we performed. This is relevant for the calculations of the integrals in Equations (4) and (5) in a region of metastability where large density fluctuations can be expected.

5. Density and structural anomalies

It is well known that the density anomaly of water is characterized by an increase of the density with temperature at constant pressure. This behaviour can be connected to the entropy through the thermodynamic relation [69]

$$\left(\frac{\partial \rho}{\partial T}\right)_P = \rho^2 \left(\frac{\partial \rho}{\partial P}\right)_T \left(\frac{\partial s}{\partial \rho}\right)_T, \tag{6}$$

owing to the stability condition (2) density anomalies are indicated by $(\partial s / \partial \rho)_T > 0$. By considering the definition of the excess entropy (3) this is equivalent to the condition [58]

$$\Sigma_{\mathrm{exc}} = \left(\frac{\partial s_{\mathrm{exc}}}{\partial \ln \rho}\right)_T > 1. \tag{7}$$

Structural anomalies are determined by the criterion [64,70,71]

$$\Sigma_{\mathrm{exc}} = \left(\frac{\partial s_{\mathrm{exc}}}{\partial \ln \rho}\right)_T > 0. \tag{8}$$

We report the two-body entropy s_2 as a function of density in Figure 4 for bulk water and in Figure 5 for the aqueous solution. For clarity only few significative

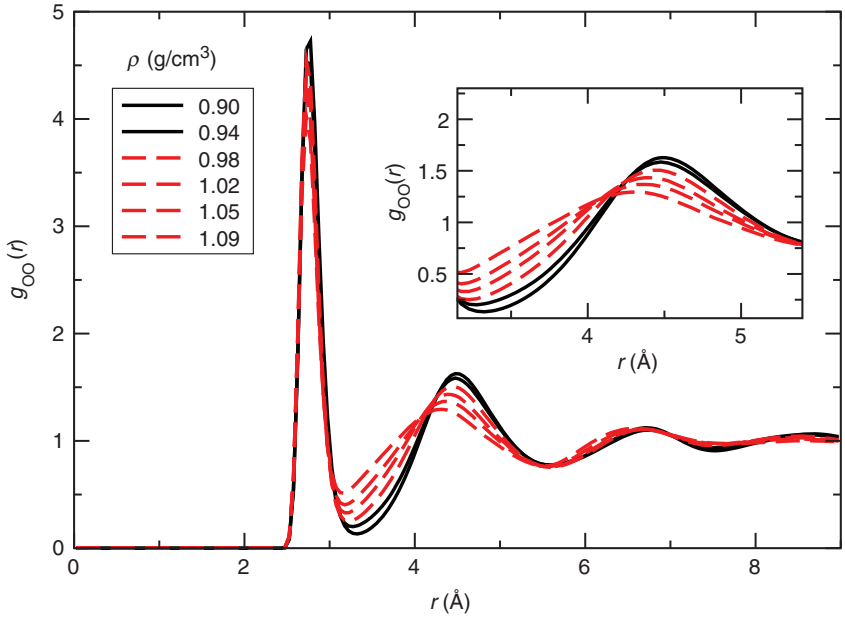

Figure 3. Oxygen–oxygen RDF of NaCl(aq) at $T = 190\,\mathrm{K}$ for various densities as indicated. The black bold curves indicate the LDL regime, while the red broken curves indicate the HDL regime. In the inset the same functions are reported on an enlarged scale in the region of the second shell. (Data from [42].)

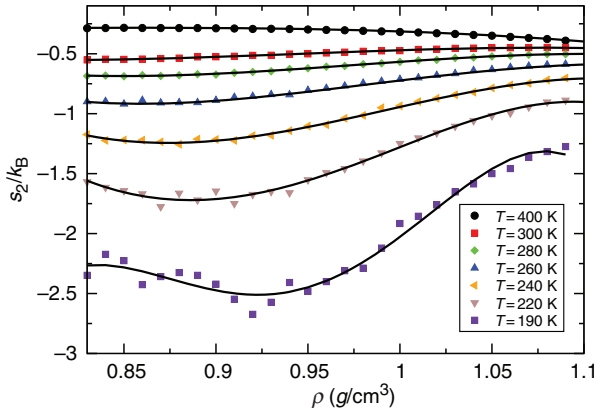

Figure 4. Two-body excess entropy s_2/k_B of bulk water calculated with Equation (4) reported as a function of density for decreasing temperatures. The bold lines are polynomial best fits.

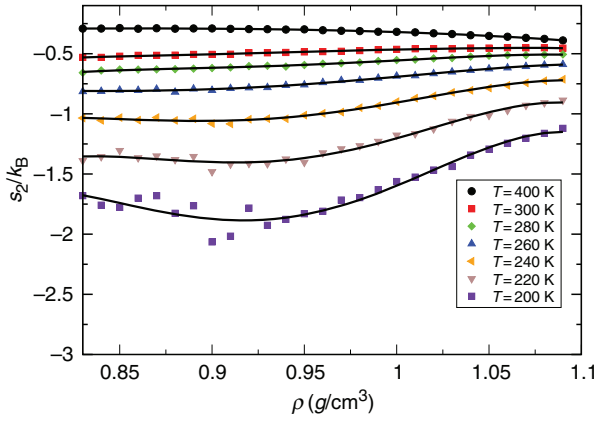

Figure 5. Two-body excess entropy s_2/k_B of NaCl(aq) calculated with Equation (5) reported as a function of density for decreasing temperatures. The bold lines are polynomial best fits.

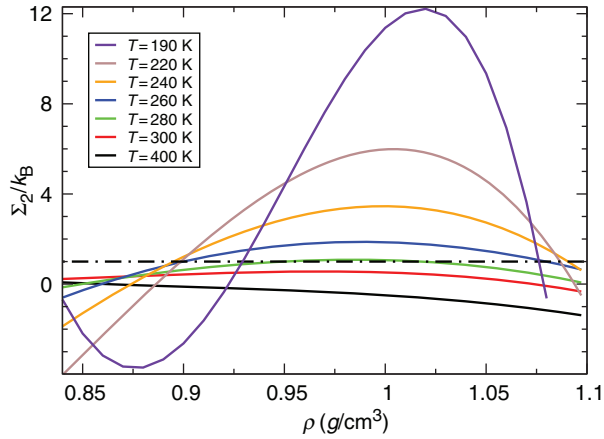

Figure 6. Function Σ_2 defined by Equation (9) for bulk water.

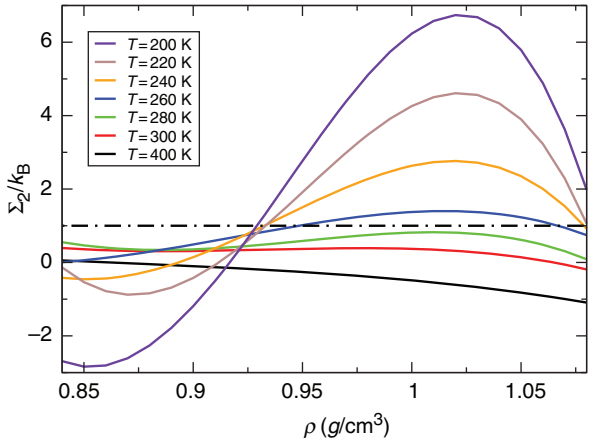

Figure 7. Function Σ_2 defined by Equation (9) for NaCl(aq).

temperatures are shown. In Figure 4 it is evident that below the temperature $T = 300$ K an anomalous behaviour of the excess entropy appears for a large range of the density. A fitting procedure to the curves made it possible to calculate the derivatives

$$\Sigma_2 = (\partial s_2/\partial \ln \rho)_T, \tag{9}$$

which are reported in Figure 6 for the bulk. The result for the temperature $T = 190$ K is likely not very accurate due to the presence of fluctuations for densities close to the LMS line. We observe that on the basis of the condition (7) the range of the density anomaly is almost correctly indicated for high temperatures but it is largely overestimated for $T = 260$ K while for $T = 190$ K at low density it is possible that the approach to the liquid instability interferes with the behaviour of the entropy.

Also the region of the structural instability determined by condition (8) is overestimated by (9), even if it can indicate the approach to the HDL stable region for low temperatures and high density. As already discussed in the literature [53,70] due to the approximations involved in calculating the excess entropy with the only two-body term s_2, the criteria $\Sigma_2 > 1$ and $\Sigma_2 > 0$ could overestimate the regions of anomalies for about 30%.

Figure 5 shows that s_2 exhibits a similar trend in the solution. The derivative Σ_2 for the ionic solution shown in Figure 7 seems to overestimate even more the region of the density anomaly, as can be seen by comparing the $T = 220$ K curves for bulk and NaCl(aq) and the respective TMD lines in Figure 1. It is possible that this is an effect of the shift of the LMS to densities closer to the TMD in the

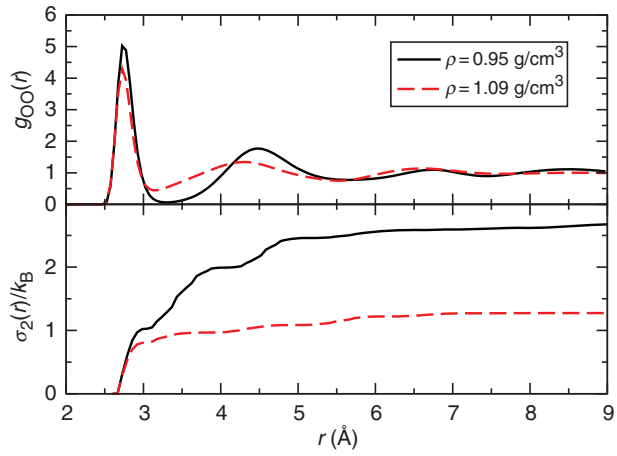

Figure 8. Bulk water. Upper panel: $g_{OO}(r)$ for $T = 190$ K and densities $0.95\,g\,cm^{-3}$ (bold black line) and $1.09\,g\,cm^{-3}$ (broken red line); bottom panel: function $\sigma_2(r)$ defined by Equation (10) for the same densities of the upper panel.

ionic solution, a point that deserves more careful investigation in the future.

In spite of some inconsistency between the predictions based on the Σ_2 criteria and the thermodynamic behaviour shown in Figure 1 the two-body excess entropy is able to give indications of the region of anomalous behaviour of water and aqueous ionic solutions.

The behaviour of the excess entropy can be related to the continuous change of structure from the LDL local structure characterized by open tetrahedral arrangement with low density and entropy to the HDL-like structure which is more compact with higher density and entropy [64]. As shown in the previous section the transformation from the LDL to the HDL form of water is characterized by the changes in the oxygen–oxygen RDF. It is interesting to study how the different coordination shells of the RDF contribute to s_2 through the integral (4). We consider the cumulative order integral [58,70]

$$\sigma_2(r) = 2\pi\rho k_B \int_0^r \{g(r')\ln[g(r')] - [g(r') - 1]\} r'^2 dr'. \tag{10}$$

From it we can estimate the contribution of each shell to $|s_2|$, of course $\sigma_2(r) \to |s_2|$ for $r \to \infty$. The results for bulk water are reported in Figure 8. In the LDL phase the first shell of the $g_{OO}(r)$ contributes almost 30% to s_2 and it is the region around the second shell that gives the main contribution. In the HDL phase the second shell is strongly modified and the first shell contributes 70% to s_2. The increase of the entropy in the HDL phase is determined by the collapse of the contribution beyond the first shell. There is evidence that the change in the structure from LDL to HDL is equivalent to a transition from a more ordered to a more disordered state in the short-range arrangement of the water molecules.

The trend does not change much for the presence of the ions, as can be seen in Figure 9. Due to the low concentration of the salt the main contribution to the entropy comes from the water RDF, but in the region beyond the first shell of the $g_{OO}(r)$ the outer shells of the g_{NaO} and g_{ClO} give some contribution to the entropy. It has recently been found [68] that at low salt concentration the water structure is almost unchanged while modifications are induced by increasing the amount of solute. It would be interesting to explore the effect on the entropy of increasing salt percentage.

6. Entropy and dynamical crossover

The excess entropy is determined by the configurational space available for a system. In this respect it can be connected also to the dynamics of the liquid. The relation between the entropy and the transport properties are based on the Rosenfeld scaling [53,57]. The idea behind the Rosenfeld scaling is that liquid diffusion is determined by the combination of collisions and cage effects and the diffusion coefficient D can be related to the excess entropy by a relation of the type [53,57]

$$D \propto \exp(\alpha s_{exc}), \tag{11}$$

where it is assumed that the cage relaxation can have a frequency proportional to the number of configurations.

A crossover in the dynamical relaxation of water from a fragile behaviour at high temperatures to a strong behaviour at low temperatures was found in experiments [72–74] and computer simulation [32,75,76]. This type of crossover was recently found also in NaCl(aq) at various ionic concentrations [77].

By taking into account relation (11) with $s_{exc} \approx s_2$ the fragile behaviour can be characterized by a Vogel–Fulcher–Tamman (VFT) function that gives

$$\frac{s_2(T)}{k_B} = A - \frac{BT_0}{T - T_0}, \tag{12}$$

where B is related to the fragility parameter. In the strong regime the function becomes of the Arrhenius type

$$\frac{s_2(T)}{k_B} = C - \frac{E}{k_B T}, \tag{13}$$

where E corresponds to an activation energy.

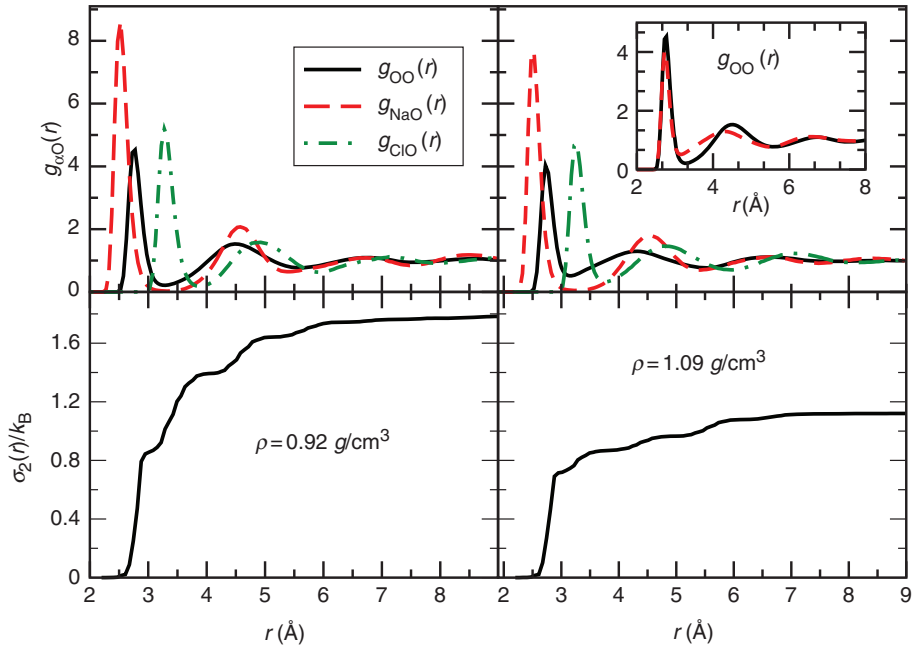

Figure 9. NaCl(aq) at $T = 200$ K. Left upper panel: $g_{\alpha o}(r)$ at density 0.92 g cm^{-3}; right upper panel: $g_{\alpha o}(r)$ at density 1.09 g cm^{-3}. Bottom panels: function $\sigma_2(r)$ defined by Equation (10) for density 0.92 g cm^{-3} on the left and density 1.09 g cm^{-3} on the right. In the inset: $g_{oo}(r)$ for 1.09 g cm^{-3} (black bold line) and for 0.92 g cm^{-3} (red broken line).

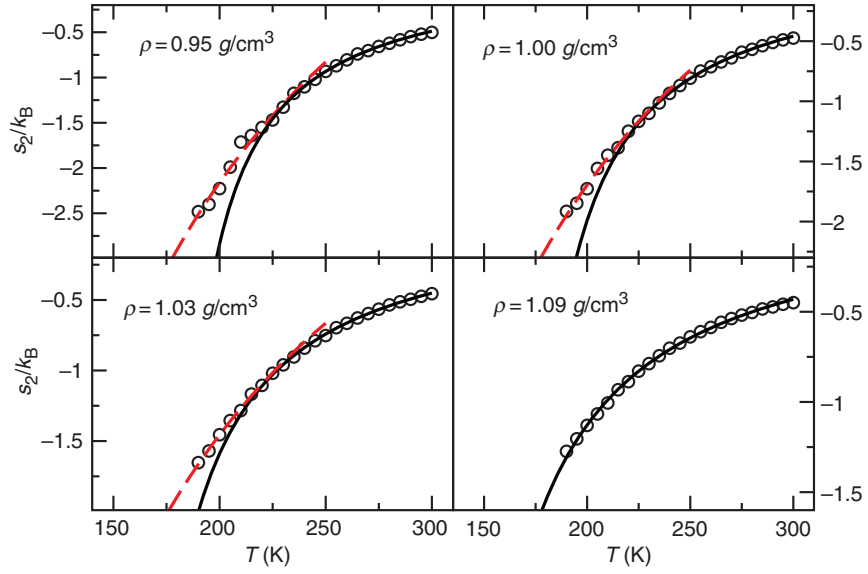

Figure 10. s_2 of bulk water as a function of temperature for four different densities, as indicated in the panels. The bold black curve is the fit to Equation (12) while the broken red curve is the fit to Equation (13).

The crossover from fragile to strong behaviour has been connected to the crossing of the Widom line approaching the liquid–liquid transformation in water [32] and polyamorphism in silica [22], but it could also be related to the hypothesis of the singularity free scenario [78]. It is of interest to investigate whether the s_{exc} could contain information on this crossover. Results obtained by fitting the behaviour at low temperature of $s_2(T)$ are shown in Figures 10 and 11 for bulk water and the salt aqueous solution respectively.

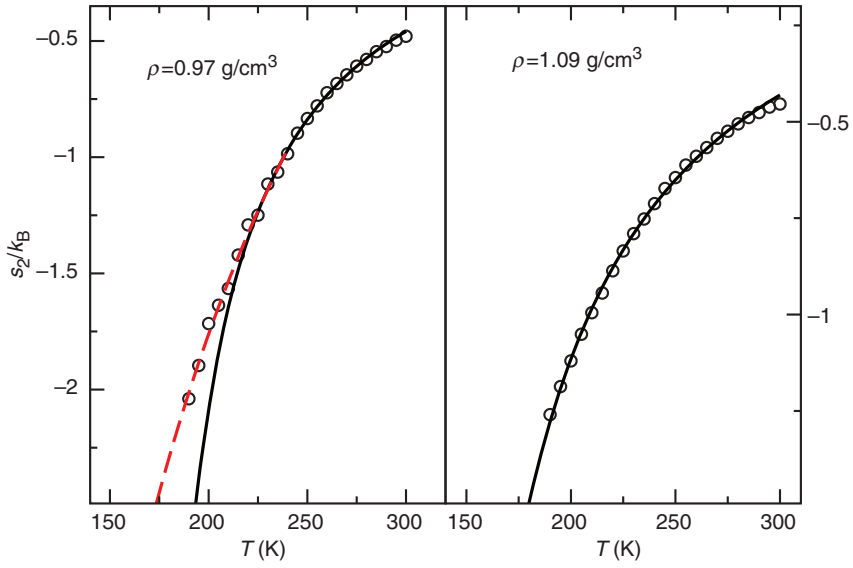

Figure 11. s_2 of the NaCl(aq) as a function of temperature for two different densities, as indicated in the panels. The bold black curve is the fit to Equation (12) while the broken red curve is the fit to Equation (13).

Table 2. Parameters of the fits to Equations (12) and (13) for bulk water and NaCl(aq).

ρ (g cm^{-3})	A	B	T_0 (K)	C	E/k_B (K)	T_{cross}
Bulk						
0.95	0.227	0.55	169.6	4.50	1332	230 ± 3
1.00	0.188	0.58	157.8	3.08	955.6	227 ± 3
1.03	0.141	0.61	148.0	2.50	790.7	220 ± 5
1.09	0.127	0.84	120.0	–	–	–
NaCl(aq)						
0.97	0.255	0.66	156.0	3.01	954.8	225 ± 5
1.09	0.185	1.06	110.1	–	–	–

It is found that in both cases the $s_2(T)$ can be fitted at high temperature with a function which corresponds to the VFT regime (12).

In the bulk, as can be seen in Figure 10, for the densities at which it is possible to cross the Widom line, reported in Figure 1, we observe a crossover to an Arrhenius behaviour (13).

For the salt solution the Widom line in Figure 1 is very flat in the ρ–T plane and this restricts the range of densities where the crossover can be observed. The behaviour of s_2 in Figure 11 is consistent with the Widom line of NaCl(aq). A strong to fragile crossover is found for the density 0.97 g cm^{-3} but not for 1.09 g cm^{-3} well inside the HDL region.

The fitting parameters for s_2 are reported in Table 2 together with the estimated crossover temperature T_{cross}. The change in the functional form of s_2 upon crossing the Widom line is consistent with the predictions about a fragile to strong crossover in water when the Widom line is crossed.

7. Conclusions

We calculated by computer simulation the excess entropy of liquid water and a salt aqueous solution in the supercooled region. We considered liquid TIP4P water both as a pure system and as a solvent in a salt solution with a NaCl concentration of 0.67 mol kg^{-1}. Previous studies [34] of both systems found a coexistence between the LDL and the HDL phases of liquid water with the presence of a LLCP. The excess entropy s_{exc} was approximated with the two-body form s_2 which can be obtained by integrating the radial distribution functions.

We found that the density and structural anomalies of both pure water and salt solution are indicated by an anomalous increase of s_2 with density. The two-body excess entropy gives an approximate estimation of the region where density and structural anomalies occur. As already observed in the literature [70], however, s_2, likely as a consequence of the two-body approximation, overestimates the density range of the anomalies of water. We found that this is true even more in the salt solution. Nevertheless it was interesting to perform a shell analysis of s_2. This analysis shows a different behaviour between the LDL and the HDL phases. In both systems in the LDL the second shell of the $g_{OO}(r)$ largely contributes to the excess

entropy while in the HDL the contribution comes substantially only from the first shell. A small correction is introduced by the outer shells of the oxygen-ion RDF. In this respect it would be of interest to explore the effect of the ionic concentration.

By relating the excess entropy to the configuration space available for diffusion we find that s_2 gives indications of a crossover from a fragile to a strong regime of the structural relaxation of supercooled liquid water. This result confirms the connection between structural and dynamical properties also in aqueous salt solutions.

This point deserves future work to investigate more deeply the relation between D and s_{exc} in this contest through the Rosenfeld scaling.

Acknowledgements

We gratefully acknowledge the computational support of CASPUR, CINECA, and the Roma Tre INFN-GRID.

References

[1] P.G. Debenedetti and H.E. Stanley, Phys. Today **56**, 40 (2003).
[2] P.G. Debenedetti, J. Phys.: Condens. Matter **15**, R1669 (2003).
[3] R.J. Speedy and C.A. Angell, J. Chem. Phys. **65**, 851 (1976).
[4] C.A. Angell, M. Oguni and W.J. Sichina, J. Phys. Chem. **86**, 998 (1982).
[5] D. Rasmussen, A. Mackenzie, C.A. Angell and J.C. Tucker, Science **181**, 342 (1973).
[6] D.E. Hare and C.M. Sorensen, J. Chem. Phys. **84**, 5085 (1986).
[7] D.E. Hare and C.M. Sorensen, J. Chem. Phys. **87**, 4840 (1987).
[8] E. Tombari, C. Ferrari and G. Salvetti, Chem. Phys. Lett. **300**, 749 (1999).
[9] Y. Xie, K.F. Ludwig Jr, G. Morales, D.E. Hare and C.M. Sorensen, Phys. Rev. Lett. **71**, 2050 (1993).
[10] P.H Poole, F. Sciortino, U. Essmann and H.E. Stanley, Nature **360**, 324 (1992).
[11] P.H. Poole, F. Sciortino, U. Essmann and H.E. Stanley, Phys. Rev. E **48**, 3799 (1993).
[12] S. Sastry, P.G. Debenedetti, F. Sciortino and H.E. Stanley, Phys. Rev. E **53**, 6144 (1996).
[13] C.A. Angell, Science **319**, 582 (2008).
[14] S. Chatterjee and P.G. Debenedetti, J. Chem. Phys. **124**, 154503 (2006).
[15] S. Sastry and C.A. Angell, Nat. Mater. **2**, 739 (2003).
[16] T. Morishita, Phys. Rev. Lett. **93**, 055503 (2003).
[17] F. Sciortino, Nat. Phys. **7**, 523 (2011).
[18] V.V. Vasisht, S. Saw and S. Sastry, Nature Phys. **7**, 549 (2011).
[19] D.J. Lacks, Phys. Rev. Lett. **84**, 4629 (2000).
[20] I. Saika-Voivod, F. Sciortino and P.H. Poole, Phys. Rev. E **63**, 011202 (2001).
[21] I. Saika-Voivod, F. Sciortino and P.H. Poole, Phys. Rev. E **69**, 041503 (2001).
[22] I. Saika-Voivod, P.H Poole and F. Sciortino, Nature **412**, 514 (2001).
[23] O. Mishima, L.D. Calvert and E. Whalley, Nature **76**, 314 (1985).
[24] R. Martonak, D. Donadio and M. Parrinello, J. Chem. Phys. **122**, 134501 (2005).
[25] K. Winkel, M. Elsaesser, E. Mayer and T. Loerting, J. Chem. Phys. **128**, 044510 (2008).
[26] C.U. Kim, B. Barstow, M.V. Tate and S.M. Gruner, Proc. Natl. Acad. Sci. U.S.A. **106**, 4596 (2009).
[27] O. Mishima and H.E. Stanley, Nature **392**, 164 (1998).
[28] O. Mishima and H.E. Stanley, Nature **396**, 329 (1998).
[29] H. Poole, I. Saika-Voivod and F. Sciortino, J. Phys.: Condens. Matter **17**, L431 (2005).
[30] M. Yamada, S. Mossa, H. Stanley and F. Sciortino, Phys. Rev. Lett. **88**, 195701 (2002).
[31] P. Jedlovszky and R. Vallauri, J. Chem. Phys. **122**, 081101 (2005).
[32] L. Xu, P. Kumar, S.V. Buldyrev, S.-H. Chen, P.H. Poole, F. Sciortino and H.E. Stanley, Proc. Natl. Acad. Sci. U.S.A. **102**, 16558 (2005).
[33] Y. Liu, A.Z. Panagiotopoulos and P.G. Debenedetti, J. Chem. Phys. **131**, 104508 (2009).
[34] D. Corradini, M. Rovere and P. Gallo, J. Chem. Phys. **132**, 134508 (2010).
[35] J.L.F. Abascal and C. Vega, J. Chem. Phys. **133**, 234502 (2010).
[36] J.L.F. Abascal and C. Vega, J. Chem. Phys. **134**, 186101 (2011).
[37] D.G. Archer and R.W. Carter, J. Phys. Chem. B **104**, 8563 (2000).
[38] R.W. Carter and D.G. Archer, Phys. Chem. Chem. Phys. **2**, 5138 (2000).
[39] O. Mishima, J. Chem. Phys. **123**, 154506 (2005).
[40] O. Mishima, J. Chem. Phys. **126**, 244507 (2007).
[41] D. Corradini, P. Gallo and M. Rovere, J. Chem. Phys. **128**, 244508 (2008).
[42] D. Corradini, M. Rovere and P. Gallo, J. Phys. Chem. B **115**, 1461 (2011).
[43] D. Corradini and P. Gallo, J. Phys. Chem. B (2011), DOI:10.1021/jp2045977.
[44] A. Baranyai and D. Evans, Phys. Rev. A **40**, 3817 (1989).
[45] L. Jorgensen, J. Chandrasekhar, J.D. Madura, R.W. Impey and M.L. Klein, J. Chem. Phys. **79**, 926 (1983).
[46] K.P. Jensen and W.L. Jorgensen, J. Chem. Theory Comput. **2**, 1499 (2006).
[47] G. Franzese and H.E. Stanley, J. Phys.: Condens. Matt. **19**, 205126 (2007).

[48] P. Kumar, S.V. Buldyrev, F.W. Starr, N. Giovambattista and H.E. Stanley, Phys. Rev. E **72**, 051503 (2005).
[49] E.G. Strekalova, M.G. Mazza, H.E. Stanley and G. Franzese, Phys. Rev. Lett. **106**, 145701 (2011).
[50] P. Gallo and M. Rovere, Phys. Rev. E **76**, 061202 (2007).
[51] J.L. Green, D.J. Durben, G.H. Wolf and C.A. Angell, Science **249**, 649 (1990).
[52] H. Kanno, R.J. Speedy and C.A. Angell, Science **189**, 880 (1975).
[53] Y. Rosenfeld, J. Phys.: Condens. Matter **11**, 5415 (1999).
[54] B.S. Jabes, M. Agarwal and C. Chakravarty, J. Chem. Phys. **132**, 234507 (2010).
[55] M. Agarwal, M. Singh, R. Sharma, M.P. Alam and C. Chakravarty, J. Phys. Chem. B **114**, 6995 (2011).
[56] R. Sharma, M. Agarwal and C. Chakravarty, Mol. Phys. **106**, 1925 (2008).
[57] J. Mittal, J.R. Errington and T.M. Truskett, J. Chem. Phys. **125**, 076102 (2006).
[58] J.R. Errington, T.M. Truskett and J. Mittal, J. Chem. Phys. **125**, 244502 (2006).
[59] A. Scala, F.W. Starr, E.L. Nave, F. Sciortino and H.E. Stanley, Nature **406**, 166 (2000).
[60] Y.D. Fomin, V.N. Ryzhov and N.V. Gribova, Phys. Rev. E **81**, 061301 (2010).
[61] M.E. Johnson and T. Head-Gordon, J. Chem. Phys. **130**, 214510 (2009).
[62] J.R. Errington and P.G. Debenedetti, Nature **409**, 318 (2001).
[63] J. Mittal, J.R. Errington and T.M. Truskett, J. Phys. Chem. B **110**, 18147 (2006).
[64] Z. Yan, S.V. Buldyrev and H.E. Stanley, Phys. Rev. E **78**, 051201 (2008).
[65] A.K. Soper, Chem. Phys. **258**, 121 (2000).
[66] C. Vega, J.L.F. Abascal, M.M. Conde and J.L. Aragones, Faraday Discuss. **141**, 251 (2009).
[67] A.K. Soper and M.A. Ricci, Phys. Rev. Lett. **84**, 2881 (2000).
[68] P. Gallo, D. Corradini and M. Rovere, Phys. Chem. Chem. Phys. **13**, 19814 (2011).
[69] R.M. Lynden-Bell and P.G Debenedetti, J. Phys. Chem. B **109**, 6527 (2005).
[70] P. Vilaseca and G. Franzese, J. Chem. Phys. **133**, 084507 (2010).
[71] H.J. Raveché, J. Chem. Phys. **55**, 2242 (1971).
[72] A. Faraone, L. Liu, C.Y. Mou, C.W. Yen and S.H. Chen, J. Chem. Phys. **121**, 10843 (2004).
[73] L. Liu, S.H. Chen, A. Faraone, C.W. Yen and C.Y. Mou, Phys. Rev. Lett. **95**, 117802 (2005).
[74] A. Faraone, K.H. Liu, C.Y. Mou, Y. Zhang and S.H. Chen, J. Chem. Phys. **130**, 134512 (2009).
[75] P. Gallo, M. Rovere and S.H. Chen, J. Phys. Chem. Lett. **1**, 729 (2010).
[76] P. Gallo, M. Rovere and S.H. Chen, J. Phys.: Condens. Matter **28**, 284102 (2010).
[77] M.P. Longinotti, M.A. Carignano, I. Szleifer and H.R Corti, J. Chem. Phys. **134**, 244510 (2011).
[78] P. Kumar, G. Franzese and H.E. Stanley, Phys. Rev. Lett. **100**, 105701 (2008).